

Research Paper

Cite this article: Zhao Y, Ren F, He L, Zhang J, Yuan Y, Xi X (2019). Design of graded honeycomb radar absorbing structure with wide-band and wide-angle properties. *International Journal of Microwave and Wireless Technologies* **11**, 143–150. <https://doi.org/10.1017/S1759078718001460>

Received: 5 June 2018

Revised: 6 October 2018

Accepted: 9 October 2018

First published online: 5 November 2018

Key words:

Effective permittivity; graded honeycomb radar absorbing structure; wide-angle; wide-band

Author for correspondence:

Xiaoli Xi, E-mail: xixiaoli@xaut.edu.cn

Design of graded honeycomb radar absorbing structure with wide-band and wide-angle properties

Yuchen Zhao¹, Fang Ren¹, Li He¹, Jinsheng Zhang^{1,2}, Yanning Yuan¹ and Xiaoli Xi¹

¹Xi'an University of Technology, Xi'an 710048, China and ²Xi'an High-tech Institute, Xi'an 710025, China

Abstract

In this paper, the design of a graded honeycomb radar absorbing structure (RAS) is presented to realize both a wide bandwidth and absorption over a wide range of angles. For both transverse-electric and transverse-magnetic polarization, a fractional bandwidth of more than 118.6% is achieved for at least a 10 dB reflectivity reduction when the incident angle is $<45^\circ$, an 8 dB reduction when the incident angle is $<55^\circ$ and a 5 dB reduction when the incident angle is $<70^\circ$. Meanwhile the 10 dB reduction upper angle limit is approximately 30° for the uniform coating honeycomb RAS in the literature, which loses its absorbing ability when the incident angle is larger than 55° . Furthermore, the total thickness of our design is 10.7 mm, which is only approximately 1.29 times that of the theoretical limitation. The good agreement between the calculated, simulated, and measured results demonstrates the validity of this optimization.

Introduction

Radar absorbing material, which is also known as RAM, is basically a material that has been specially designed and shaped to absorb incident microwave radiation in the radar operation frequency band [1–3]. In its early stages of development, the RAMs usually suffered from several practical problems, such as a narrow frequency band and incident angle sensitivity [4]. Hence, in the past few decades, there has been an increasing demand for high-performance RAM with wide-band and wide-angle properties for various military and civilian applications.

Until now, many different techniques, such as the frequency-selective surface (FSS) and the plasma, have been developed to meet this requirement [5–8]. Among these techniques, the honeycomb radar absorbing structure (RAS), which is characterized by its light weight, good strength, low density, and low dielectric constant, provides one of the greatest potentials for achieving excellent load bearing and electromagnetic energy absorbing capabilities [9]. Over the past decades, abundant studies have been carried out to understand and improve the electromagnetic behaviors for such an important structure, which are mostly on the honeycomb with a novel unit-cell structure [10–15], absorbent application and broadband optimization [15–17], full-wave analysis approach [18, 19], effective electromagnetic parameters [20–25], novel design methods [26, 27], and so on. However, compared with other techniques, especially artificial electromagnetic structures, such as the FSS absorber, only a few works concerning the oblique incident performance have been reported for the honeycomb RAS. In [28], the reflectivity of some honeycomb panels at an incident angle of 45° and with horizontal polarization was tested and the results show that the reflectivity is better than -20 dB over the whole range of 4–18 GHz. However, the absence of data for the vertical polarization and the larger incident angle make it impossible to conduct a comprehensive assessment of its wide-angle property. More detailed results for hexagonal and overexpanded honeycomb RASs can be found in [29] and [30]. According to these two works, the transverse-magnetic (TM) polarization has a better wide-angle property than the transverse-electric (TE) polarization. Specifically, for a 30 mm-thick hexagonal honeycomb, a reduction in reflection of at least a 10 dB in the range of 4.6–18 GHz can be achieved for TM polarization when the incident angle is less than approximately 50° (only 25° for TE polarization). Furthermore, the honeycomb RAS will lose its radar absorbing ability and become a radar reflective structure when the incident angle is larger than 55° .

Although the existing data provide good guidance for the application of the honeycomb RAS, we are still not sure whether this will be its ultimate limit for realizing both a wide bandwidth and absorption over a wide range of angles. Recently, the graded design of the coating thickness of the honeycomb RAS was reported in [31, 32]. Then, we presented a novel design method for their graded idea based on our dispersive closed-form expression for the effective permittivity of the honeycomb RAS [33]. In this study, the dispersive effective permittivity formula can reduce the computational error of reflectivity by approximately 75%, and the

optimizer with a normal incident objective function for wide-band application is utilized to achieve a fractional bandwidth of 141.2%, i.e., 3.1–18 GHz, for at least a 10 dB reflectivity reduction. Compared with the uniform coating technique, the graded coating design not only provides a better wide-band property but also reduces the thickness of the honeycomb RAS. Although these efforts focus only on the normal incident situation, it offers an opportunity to develop the design possibilities for the honeycomb RAS with wide-band and wide-angle properties.

In this paper, we present a graded honeycomb RAS design to develop better oblique incident performance. For both TE and TM polarization, the optimized honeycomb RAS has a fractional bandwidth of 118.6% for at least 10, 8, and 5 dB reflectivity reductions when the incident angle is $<45^\circ$, 55° , and 70° , respectively. The total thickness of our design is 10.7 mm, which is only approximately 1.29 times the theoretical limitation. Meanwhile, for a 10 dB reflectivity reduction, the thickness in terms of that at the lowest cut-off frequency decreases by 59% and the thickness-to-bandwidth ratio increases by 134% compared with the honeycomb RASs in [29] and [30]. A good agreement between the calculated, simulated, and measured data demonstrates the validity of the optimization results. In addition, although there have not been much geometric differences between the proposed configuration and that presented in [33] due to the very limited design variable database, the choice of an objective function that takes both the bandwidth and incident angle into account improves the oblique incident performance of graded honeycomb RAS. More importantly, a comprehensive comparison between different optimization results reveals that the combination of a proper objective function and a smart coating approach produces the best honeycomb RAS, but if one has to make a choice, a better coating technique will improve the performance of the honeycomb RAS more effectively.

Graded honeycomb RAS design

Design methodology

The geometry of the honeycomb RAS is illustrated in Fig. 1. The honeycomb can be considered a two-phase medium, including the background phase (the effective medium of honeycomb frame and air) and the absorbent phase (the RAM coating). The unit-cell structure is a standard hexagon. The incident angle is θ for the plane wave.

There are three key steps in the design of the graded honeycomb RAS [33]. First, an electromagnetic field analysis method is selected to efficiently analyze and evaluate all possible solutions. Second, a proper multi-layer model should be chosen, which has to be flexible enough to describe various graded profiles. Finally, a suitable objective function must be defined for a particular application. After fulfilling these tasks, optimizations are run to produce the honeycomb structures, which are expected to perform optimally. In the following, each of the above steps is discussed.

Analysis method

Since the field interaction with the honeycomb RAS needs to be solved many times during the whole process, the analysis method should be efficient enough to make numerical optimizations possible. Additionally, because of the numerical cancellations in the computation of small values, a high accuracy analysis method is

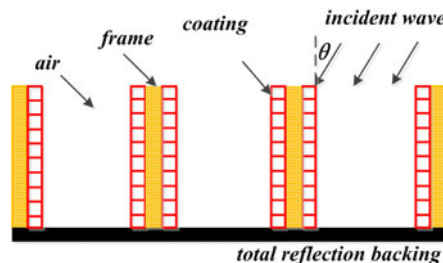


Fig. 1. The geometry of honeycomb RAS.

of utmost importance. The full-wave numerical means, though accurate, are complicated and time-consuming. The classic Hashin–Shtrikman (HS) homogenization theory, though easy to use, ignores the influence of the frequency of the incident wave and may lead to noticeable errors in calculating the effective permittivity in a wide frequency band. Therefore, the following dispersive closed-form expressions for axial permittivity ε_z and the axial permittivity ε_t of the honeycomb RAS are used for our optimization.

$$\varepsilon_t = \varepsilon_g \left[1 + 4 \frac{\varepsilon_g^* U}{\varepsilon_g} \right], \quad (1)$$

$$\varepsilon_z = g\varepsilon_a + (1 - g)\varepsilon_b, \quad (2)$$

where the asterisk (*) stands for the conjugation, ε_a and g are the permittivity and fractional volume of the absorbent phase, respectively, ε_b and $1 - g$ are the permittivity and fractional volume of the background phase, respectively, and U is the dispersion characteristic part and its derivation can be found in [24] and [33].

Multi-layer model

The creation of continuously changing RAM coating is inherently impossible, although in theory, one can use a multi-layer model with a very fine-scaled unit layer structure to approach a continuous approximation. Hence, it is more practical to work with a relatively large unit layer. However, the lack of prior knowledge about the coating profile makes it very difficult to determine the number and thickness of the unit layer that are needed to avoid large errors when a continuous profile is transformed to a discretized one.

According to our experience, the combination of a relatively large number and flexible thickness range with small lower limit and large upper limit is a suitable choice of parameters for the unit layer structure. As a result, the whole honeycomb is divided into 10 unit layers and the thickness for each layer is set to be >0.1 mm and <2.5 mm.

Objective function

Different from our previous design, a honeycomb RAS that has an optimum bandwidth and angular stability within the intervals of 2–18 GHz and $0-90^\circ$, respectively, is to be obtained in this work. Hence, an oblique incident objective function is defined for wide-band and wide-angle optimization.

First, two two-dimensional (2D) matrixes, M^{TE} and M^{TM} , are generated to discretely decompose the continuous optimization domain for TE and TM polarization. The size of these frequency-angle matrixes is $N_f \times N_\theta$, where $N_f = 65$ is the number of frequency points with equal intervals in the range of 2–18 GHz and $N_\theta = 19$ is the number of angles with an equal interval in the range of 0–90°. Second, all the elements in M^{TE} and M^{TM} are initially set to be 0 and the corresponding element in which the optimized reflectivity R^{TE} or R^{TM} is below a desired value R_0 will be switched to 1, namely,

$$M_{rs}^p = \begin{cases} 1 & R^p \leq R_0 \\ 0 & R^p > R_0 \end{cases}, \quad (3)$$

where the superscript p is TE or TM , the subscripts r and s are integers that represent the positional index of a matrix element, and, considering the possible error of the calculated effective permittivity, R_0 is set to be -11 dB. Then, the object function can be described as follows for different design goals.

For the TE or TM polarization design, the objective function is given by (4a) and (4b), respectively.

$$objective = \max \left\{ \sum_{r=1}^{N_f} \sum_{s=1}^{N_\theta} M_{rs}^{TE} / (N_f \times N_\theta) \right\}, \quad (4a)$$

$$objective = \max \left\{ \sum_{r=1}^{N_f} \sum_{s=1}^{N_\theta} M_{rs}^{TM} / (N_f \times N_\theta) \right\}. \quad (4b)$$

For polarization-independent design, the following oblique incident object function will be considered

$$objective = \max \left\{ \sum_{r=1}^{N_f} \sum_{s=1}^{N_\theta} (M_{rs}^{TE} \times M_{rs}^{TM}) / (N_f \times N_\theta) \right\}. \quad (5)$$

Since polarization independence is the basic requirement of the oblique incident design of the honeycomb RAS, the TE and TM polarization will be treated equally in this work. Therefore, this polarization-independent objective function will be used in the optimization process.

Design result

In this part, the particle swarm optimization is employed to pursue the desired performance for the honeycomb RAS. The design result is made up of four honeycomb panels, which are formed by the multi-layer model with 10 unit layers. From the top to the bottom, the layer thickness and coating thickness are 5.4 and 0.16, 1.0 and 0.40, 3.3 and 0.66, and 1.0 and 0.28 mm, respectively, as shown in Fig. 2.

To better demonstrate the wide-band and wide-angle properties of this graded design, the 3D plots and contour plots (in dB unit) of the optimized reflectivity are illustrated in Figs 3(a) and 3(b) for TM polarization, and Figs 3(c) and 3(d) for TE polarization. As seen from the curves in the figure, for both TE and TM polarization, the fractional bandwidth of more than 118.6%, i.e., the range of 4.6–18 GHz, is achieved for at least a 10 dB reflectivity reduction when the incident angle is $<45^\circ$, an 8 dB reduction when the incident angle is $<55^\circ$, and a 5 dB

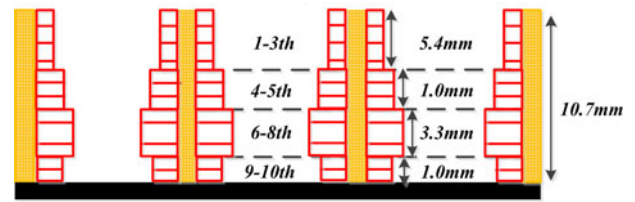


Fig. 2. The graded honeycomb RAS design result.

reduction when the incident angle is $<70^\circ$. Meanwhile the 10 dB reduction upper angle limit is approximately 25° and 30° for the uniform coating hexagonal and overexpanded honeycomb RASs in [29] and [30], which lose their absorbing ability when the incident angle is larger than 55° . In addition, the total thickness is 10.7 and 30 mm for our graded design and the uniform design in the literature, which indicates that the graded coating is a better choice for the ultra-thin honeycomb RAS. A more detailed comparison between our design and the theoretical limitation will be discussed in the next section.

Verification and comparisons

Verification

The measured effective permittivity (available in the range of 8–12 GHz), the dispersive effective permittivity formula, and the commercial full-wave simulation software are utilized to further demonstrate the validity of our optimization, as shown in Fig. 4.

According to the figure, the reflectivity curves obtained by the calculated, simulated, and measured data are in good agreement with each other. This proves the correctness of our design.

Comparisons

Although our design has better oblique incident performance than the honeycombs in the literature, the optimization process itself does not provide any criterion for evaluating how good the resulting design is. Hence, the theoretical limitation for creating broad-band non-magnetic absorbers should be derived to further evaluate the presented honeycomb RAS.

Since the considered honeycomb absorbers are constructed from non-magnetic, linear, passive, and time-invariant materials, the limitations for Γ_{TE} and Γ_{TM} , i.e., the reflection coefficients for TE and TM polarization, are given by [34]

$$\int_0^\infty \omega^{-2} \log \left| \frac{1}{\Gamma_{TE}(j\omega)} \right| d\omega \leq \frac{\pi d \cos \theta}{c}, \quad (6a)$$

$$\int_0^\infty \omega^{-2} \log \left| \frac{1}{\Gamma_{TM}(j\omega)} \right| d\omega \leq \frac{\pi d}{c \cos \theta}, \quad (6b)$$

where d is the total thickness of the honeycomb RAS, j is the square root of -1 , and c is the speed of light in a vacuum. The inequalities (6a) and (6b) establish the fundamental limits for the performance of any physically realizable passive absorber backed by a ground plane. Notably, they are simple expressions involving the total thickness and incident angle.

In the absorption band, the reflection coefficient is designed to be less than a desired value Γ_0 , for instance, 0.1, 0.158, and 0.316

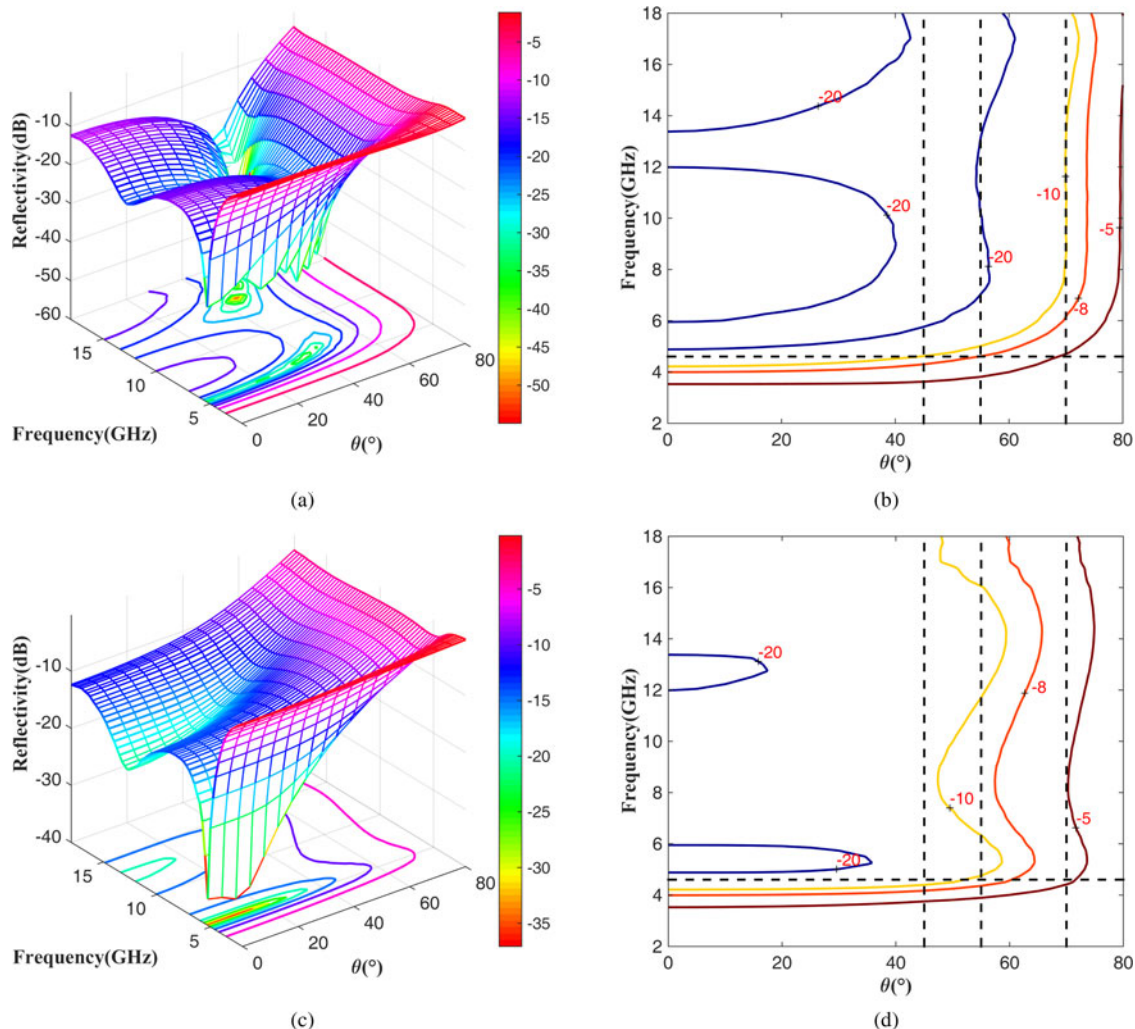


Fig. 3. Reflectivity of the optimized graded honeycomb RAS.

for at least 10, 8, and 5 dB reflectivity reductions, respectively. Therefore, a piecewise linear approximation of the frequency response can be a simple candidate to evaluate the theoretical limitation. In this way, the desired reflection coefficient can be expressed as

$$\Gamma_p(f) = \begin{cases} \Gamma_0 & f_{\min} < f < f_{\max} \\ 0 & \text{else} \end{cases}, \quad (7)$$

where p stands for the polarization, i.e., TE or TM, and f_{\max} and f_{\min} are the upper and lower frequency limit of the absorption band, respectively.

Tables 1 and 2 display the detailed comparison between our design and the reported uniform coating honeycomb RAS in [29] and [30]. It can be found that the total thickness of our design is only approximately 1.29 times of the theoretical limitation. Compared with the results in the literature, the thickness in term of the wavelength at the lowest cut-off frequency d/λ_{\max} is decreased by 59%, the thickness to bandwidth ratio $(\lambda_{\max} - \lambda_{\min})/d$ is increased by 134%, and the angular stability range is increased by 50, 44, and 55% for at least 10, 8, and 5 dB reflectivity reductions, respectively.

Furthermore, the optimization results for different coating techniques, which are obtained by using the same optimization variables and settings, are compared in Table 3. The total thickness of uniform honeycomb RAS is more than two times that of the graded coating honeycomb. The best objective value is 0.543 for the graded coating and 0.465 for the uniform coating. Meanwhile, to achieve the same angular stability, i.e., at least 10, 8, and 5 dB reflectivity reductions in the ranges of 0–45°, 0–55°, and 0–70°, respectively, the absorption bandwidth decreases from 13.4 to 11.1 GHz. In addition, although the absorption in the S-band (2–4 GHz) benefits from its large thickness, the uniform coating structure still suffers from an undesired operation band gap in the range of 3.4–8.0 GHz, as illustrated in Fig. 5.

Finally, the presented honeycomb RAS will be further evaluated by comparison with our previous graded coating design in [33]. The 10 dB reflectivity reduction contour lines are displayed in Figs 6(a) and 6(b). The presented honeycomb RAS has better angular stability and polarization-independence property, but its bandwidth is less than the previous design. Because the selection of the objective function is the main difference between these two works, it indicates that the normal incident objective function itself can only provide good absorption for the TM polarization wave, while the optimization for the TE polarization wave needs

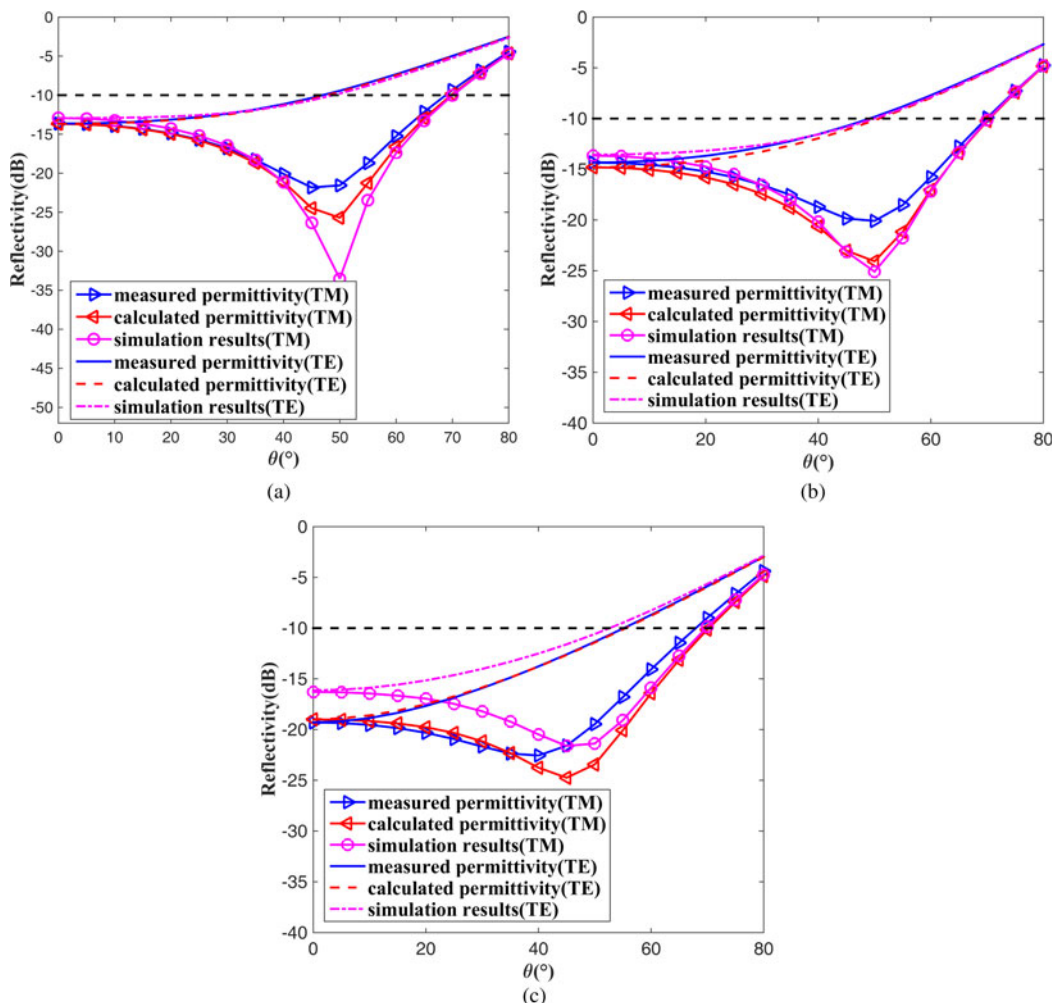


Fig. 4. Validity of our optimization.

Table 1. Wide-band property comparison with [29] and [30] (at least 10 dB reflectivity reduction)

Absorber	d (mm)	d/λ_{max}	$(\lambda_{max} - \lambda_{min})/d$
Theoretical limitation	8.2	0.123	6.07
Our design	10.7	0.164	4.54
[29]	30	0.46	1.62
[30]	30	0.40	1.94

Table 2. Wide-angle property comparison with [29] and [30] (at least 10, 8, and 5 dB reflectivity reductions)

Absorber	10 dB reduction	8 dB reduction	5 dB reduction
Our design	0–45°	0–55°	0–70°
[29]	0–25°	0–30°	0–35°
[30]	0–30°	0–38°	0–45°

Table 3. Comparison between graded and uniform coating

Coating type	d (mm)	Operation band (GHz)	Bandwidth (GHz)
Graded	10.7	4.6–18	13.4
Uniform	24.7	2.3–3.4 and 8–18	11.1

an objective function that takes both the bandwidth and incident angle in to account. In addition, as shown in Fig. 6(c), the oblique incident objective value is 0.543 for the presented honeycomb RAS, 0.497 for the graded design in [33], and 0.465 for the uniform coating. Obviously, on the one hand, one can obtain the best solution when the oblique incident objective function and graded coating are used together. On the other hand, the combination of the graded coating and normal incident objective function can provide better result than the uniform coating approach combined with the oblique incident objective function. This means that both the objective function and the coating technique are of importance for the design of the honeycomb RAS with wide-band and wide-angle properties, but a smart coating strategy plays a greater role than a good objective function.

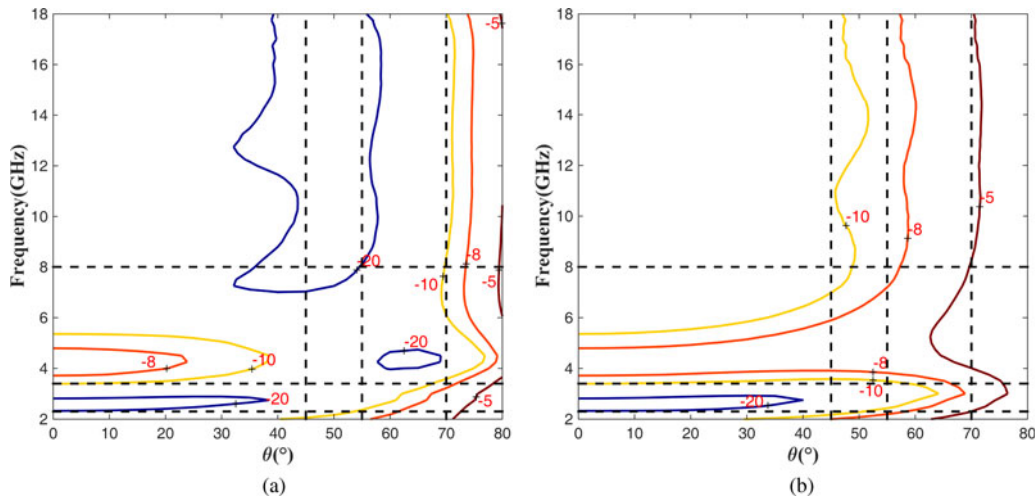


Fig. 5. Uniform coating optimization results.

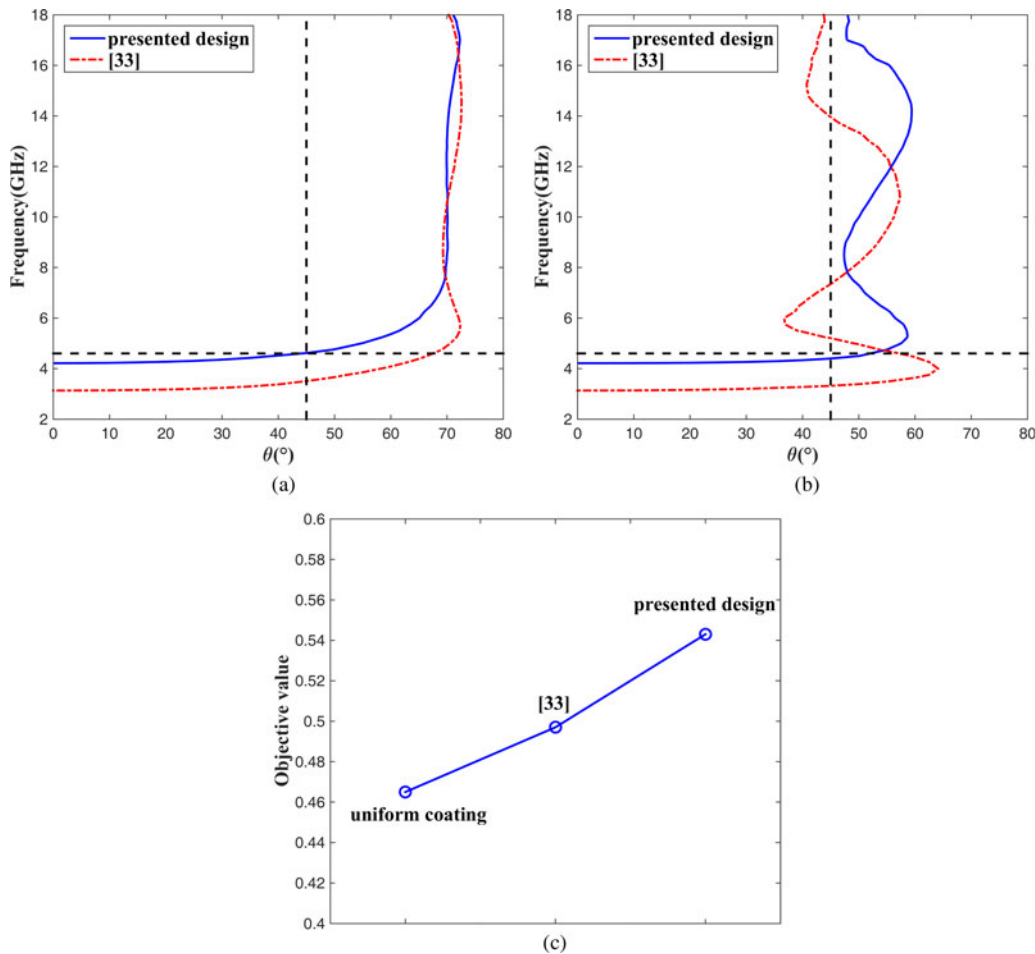


Fig. 6. Comparison with [33].

Conclusion

In summary, we present a coating thickness optimization of the graded honeycomb RAS for the wide-band and wide-angle

application. The fractional bandwidth of more than 118.6% is achieved for at least a 10 dB reflectivity reduction when the incident angle is $<45^\circ$, an 8 dB reduction when the incident angle is $<55^\circ$, and a 5 dB reduction when the incident angle is $<70^\circ$. The

optimized solution is much better than the available results in the literature and the good agreement between the calculated, simulated, and measured data demonstrates the validity of our optimization. Finally, a detailed comparison shows that the selection of the coating technique, rather than the choice of the objective function, can improve the performance of the honeycomb RAS more effectively.

Acknowledgement. This work was partly supported by the National Natural Science Foundation of China under project numbers 61501369, 21706208, and 51773167, the Postdoctoral Foundation of China under project number 2016M592904XB, the Shaanxi Province Natural Science Foundation Research Project under project number 2017JM6081, the Young Talent fund of University Association for Science and Technology in Shaanxi China under project number 20170110, the Postdoctoral Research Project of Shaanxi Province under project number No.2016BSHEDZZ36, Xi'an Science and Technology Plan Project under project number 2017080CG/RC043 (XALG013), and the Foundation of Xi'an University of Technology under project numbers 105-211423, 2016CX040, 310-252051618.

References

- Choi I, Lee DY and Lee DG (2015) Radar absorbing composite structures dispersed with nano-conductive particles. *Composite Structures* **122**, 1171–1177.
- Nam YW, Choi JH, Lee WJ and Kim CG (2017) Thin and lightweight radar-absorbing structure containing glass fabric coated with silver by sputtering. *Composite Structures* **160**, 1171–1177.
- Teber A, Unver I, Kavas H, Aktas B and Bansal R (2016) Knitted radar absorbing materials (RAM) based on nickel-cobalt magnetic materials. *Journal of Magnetism and Magnetic Materials* **406**, 228–232.
- Ghayekhloo A, Afsahi M and Orouji AA (2017) Checkerboard plasma electromagnetic surface for wideband and wide-angle bistatic radar cross section reduction. *IEEE Transactions on Plasma Science* **45**, 603–609.
- Mishra N, Khusboo K and Chaudhary RK (2018) An ultra-thin polarization independent quad-band microwave absorber-based on compact metamaterial structures for EMI/EMC applications. *International Journal of Microwave and Wireless Technologies* **10**, 422–429.
- D'Elia UF, Pelosi G, Selleri S and Taddei R (2010) A carbon-nanotube-based frequency-selective absorber. *International Journal of Microwave and Wireless Technologies* **10**, 479–485.
- Shen Y, Pei Z, Pang Y, Wang J, Zhang A and Qu S (2015) Phase random metasurfaces for broadband wide-angle radar cross section reduction. *Microwave and Optical Technology Letters* **52**, 2813–2819.
- Ayop O, Rahim MKA, Murad NA and Samsuri NA (2016) Dual-resonant polarization-independent and wide-angle metamaterial absorber in X-band frequency. *Applied Physics A: Solids and Surfaces* **122**, 374.
- Smith FC (1999) Effective permittivity of dielectric honeycombs. *IEE Proceedings – Microwaves, Antennas and Propagation* **146**, 55–59.
- Smith FC and Scarpa F (2004) Design of honeycomb-like composites for electromagnetic and structural applications. *IEE Proceedings – Science, Measurement and Technology* **151**, 9–15.
- Chen MJ, Pei YM and Fang DN (2010) Computational method for microwave absorbing structures with 2-D Kagome lattice grids. *International Journal of Applied Electromagnetics* **33**, 1691–1694.
- Smith FC, Scarpa F and Chambers B (2000) The electromagnetic properties of re-entrant dielectric honeycombs. *IEEE Microwave and Optical Technology Letters* **10**, 451–453.
- Kopyt P, Damian R, Celuch M and Ciobanu R (2010) Dielectric properties of chiral honeycombs – modelling and experiment. *Composites Science and Technology* **70**, 1080–1088.
- Ciobanu R, Damian R and Casian-Botez I (2010) Electromagnetic characterization of chiral auxetic metamaterials for EMC applications. *Computer Standards & Interfaces* **32**, 101–109.
- Xie S, Ji ZJ, Yang Y, Hou GY and Wang J (2016) Electromagnetic wave absorption properties of honeycomb structured plasterboards in S and C bands. *Journal of Building Engineering* **7**, 217–233.
- He YF, Gong RZ, Cao H, Wang X and Zheng Y (2007) Preparation and microwave absorption properties of metal magnetic micropower-coated honeycomb sandwich structures. *Smart Materials and Structures* **16**, 1501–1505.
- Khurram AA, Ali N, Rakha SA, Zhou PH and Munir A (2014) Optimization of the carbon coating of honeycomb cores for broadband microwave absorption. *IEEE Transactions on Electromagnetic Compatibility* **56**, 1061–1065.
- Chen MJ, Pei YM and Fang DN (2009) Computational method for radar absorbing composite lattice grids. *Computational Materials Science* **46**, 591–594.
- Ouchetto O, Majd BAE, Ouchetto H, Essakhi B and Zouhdi S (2016) Homogenization of periodic structured materials with chiral properties. *IEEE Transactions on Antennas and Propagation* **64**, 1751–1758.
- Quiévy N, Bollen P, Thomassin JM, Detrembleur C, Pardoën T, Bailly C and Huynen I (2012) Electromagnetic absorption properties of carbon nanotube nanocomposite foam filling honeycomb waveguide structures. *IEEE Transactions on Electromagnetic Compatibility* **54**, 43–51.
- Zhou PH, Huang LR, Xie JL, Liang DF, Lu HP and Dong LJ (2012) A study on the effective permittivity of carbon/PI honeycomb composites for radar absorbing design. *IEEE Transactions on Antennas and Propagation* **60**, 3679–3683.
- Qiu KP, Feng SQ, Wu C, Zhang WH and Liu ZJ (2016) Calculation of effective permittivity and optimization of absorption property of honeycomb cores with absorbing coatings. *Materials Science (Medžiagotyra)* **22**, 318–322.
- Liu L, Fan CZ, Zhu NB, Zhao ZY and Liu RP (2014) Effective electromagnetic properties of honeycomb substrate coated with dielectric or magnetic layer. *Applied Physics A: Materials* **116**, 901–905.
- Zhao YC, Liu JF, Song ZG and Xi XL (2016) Novel closed-form expressions for effective electromagnetic parameters of honeycomb radar absorbing structure. *IEEE Transactions on Antennas and Propagation* **64**, 1768–1778.
- Johansson M, Holloway CL and Kuester EF (2005) Effective electromagnetic properties of honeycomb composites, and hollow-pyramidal and alternating-wedge absorbers. *IEEE Transactions on Antennas and Propagation* **53**, 728–736.
- Choi WH, Shin JH, Song TH, Lee WY, Lee WJ and Kim CG (2016) Design of broadband microwave absorber using honeycomb structure. *Electronics Letters* **50**, 292–293.
- Choi WH and Kim CG (2015) Broadband microwave-absorbing honeycomb structure with novel design concept. *Composites Part B: Engineering* **83**, 14–20.
- Fan HL, Yang W and Chao ZM (2007) Microwave absorbing composite lattice grids. *Composites Science and Technology* **67**, 3472–3479.
- Feng J, Zhang YC, Wang P and Fan HL (2016) Oblique incidence performance of radar absorbing honeycombs. *Composites Part B: Engineering* **99**, 465–471.
- Wang P, Zhang YC, Chen H, Zhou Y, Jin F and Fan HL (2018) Broadband radar absorption and mechanical behaviors of bendable over-expanded honeycomb panels. *Composites Science and Technology* **162**, 33–48.
- Zhou PH, Huang LR, Xie JL, Liang DF, Lu HP and Dong LJ (2015) Prediction of microwave absorption behavior of graded honeycomb composites based on effective permittivity formulas. *IEEE Transactions on Antennas and Propagation* **63**, 3496–3501.
- Rinaldi A, Proietti A, Tamburrano A and Sarto MS (2018) Graphene-coated honeycomb for broadband lightweight absorbers. *IEEE Transactions on Electromagnetic Compatibility* **60**, 1454–1462.
- Zhao YC, Liu JF, Song ZG and Xi XL (2017) Novel design method for graded honeycomb radar absorbing structure based on dispersive effective permittivity formula. *IEEE Antennas and Wireless Propagation* **16**, 1281–1284.

34. Doane JP, Sertel KS and Volakis JL (2013) Matching bandwidth limits for arrays backed by a conducting ground plane. *IEEE Transactions on Antennas and Propagation* **61**, 2511–2518.



Yuchen Zhao received the B.S., M.S., and Ph.D. degrees in Electronic Science and Technology from Northwestern Polytechnical University, Xi'an, China, in 2007, 2010, and 2014, respectively. He joined the faculty of Electronic Engineering Department, Xi'an University of Technology, in 2014. His research interests include antenna and wave propagation.



Fang Ren received her diploma in 2010 from the Xi'an University of Technology and received her Ph.D. degree in Chemistry at the Northwestern Polytechnical University in 2015. Her main research interest is electromagnetic shielding.



Li He was born in Shaanxi, China. He received the doctorate in Electronic Science and Technology from Xi'an Jiaotong University, Xi'an, China, 2015. He became a full-time teacher in Xi'an University of Technology in 2015, Xi'an, China. His main research interests are electromagnetic absorption materials.



Jinsheng Zhang received the M.S. and Ph.D. degrees in Navigation, Guidance, and Control from the Xi'an Research Institute of Hi-tech, Xi'an, China, in 2005 and 2009. In 2009, he joined the control faculty of the Xi'an Research Institute of Hi-tech, Xi'an, China, where he founded the geomagnetic matching navigation research team in 2004. He currently works as an engineer and his recent research interests include geomagnetic matching navigation, simulation and evaluation, and wave propagation.



Yanning Yuan received the B.S. degree in Electronic Information from Liaoning Shihua University, Fushun, China, in 2004, M.S. degree in Communicating Engineering from Xi'an University of Technology, Xi'an, China, in 2007. She joined the Shaanxi Lingyun Science and Technology Co., Ltd. and served as a project manager subsequently. She is currently a full-time research worker at the Xi'an University of Technology. Her research interests include ultra-wideband antennas, multi-frequency antenna, and RF circuit.



Xiaoli Xi received the B.S. degree in Applied Physics from the University of Defense Technology, Changsha, China, in 1990. M.S. degree in Biomedical Engineering from Fourth Military Medical University, Xi'an, China, in 1998, and Ph.D. degree in Electrical Engineering from Xi'an Jiaotong University, Xi'an, China, in 2004. She is currently a Professor at the Department of Electric Engineering, Xi'an University of Technology, Xi'an, China. Her recent research interests include wave propagation, antenna design, and communication signal processing.

Jinsheng Zhang received the M.S. and Ph.D. degrees in Navigation, Guidance, and Control from the Xi'an Research Institute of Hi-tech, Xi'an, China, in 2005 and 2009. In 2009, he joined the control faculty of the Xi'an Research Institute of Hi-tech, Xi'an, China, where he founded the geomagnetic matching navigation research team in 2004. He currently works as an engineer and his recent research interests

Yanning Yuan received the B.S. degree in Electronic Information from Liaoning Shihua University, Fushun, China, in 2004, M.S. degree in Communicating Engineering from Xi'an University of Technology, Xi'an, China, in 2007. She joined the Shaanxi Lingyun Science and Technology Co., Ltd. and served as a project manager subsequently. She is currently a full-time research worker at the Xi'an University of

Xiaoli Xi received the B.S. degree in Applied Physics from the University of Defense Technology, Changsha, China, in 1990. M.S. degree in Biomedical Engineering from Fourth Military Medical University, Xi'an, China, in 1998, and Ph.D. degree in Electrical Engineering from Xi'an Jiaotong University, Xi'an, China, in 2004. She is currently a Professor at the Department of Electric